JOURNAL OF MATERIALS SCIENCE 27 (1992) 255–262

Preparation of $SiB_{4\pm x}$ and SiB_6 plates by chemical vapour deposition of $SiCl_4 + B_2H_6$ system

MASAKAZU MUKAIDA, TAKASHI GOTO, TOSHIO HIRAI
Institute for Materials Research, Tohoku University, 2-1-1 Katahira Sendai 980, Japan

$SiB_{4\pm x}$ and SiB_6 plates were prepared by chemical vapour deposition (CVD) using $SiCl_4$, B_2H_6 and H_2 gases under the conditions of deposition temperatures (T_{dep}) from 1323–1773 K, total gas pressures (P_{tot}) from 4–40 kPa and B/Si source gas ratio ($m_{B/Si} = 2B_2H_6/SiCl_4$) from 0.2–2.8. The effects of CVD conditions on the morphology, structure and composition of the deposits were examined. High-purity and high-density $SiB_{4\pm x}$ and SiB_6 plates about 1 mm thick were obtained at the deposition rates of 71 and 47 nm s^{-1}, respectively. The lattice parameter, composition and density of CVD $SiB_{4\pm x}$ plates were dependent on their non-stoichiometry. The lattice parameter, a, was 0.6325 nm, but c ranged from 1.262–1.271 nm. The B/Si atomic ratio ranged from 3.1–5.0, and the density ranged from $2.39–2.45 \times 10^3$ kg m^{-3}. The CVD SiB_6 plates showed constant values of lattice parameters ($a = 1.444$ nm, $b = 1.828$ nm, $c = 0.9915$ nm), composition (B/Si = 6.0) and density (2.42×10^3 kg m^{-3}), independent of CVD conditions.

1. Introduction

Many compounds such as SiB_3 [1], SiB_4 [2], SiB_6 [1, 3] and SiB_n (n = 14, 15, 40, etc.) [4] are known in the Si–B system. In past reports [1, 2], SiB_3 and SiB_4 have been considered to be the same compound, having a structure of space group D^5_{3d}-R3m, like B_4C [5]. It remains uncertain whether the correct nomenclature should be SiB_3 or SiB_4. The difference between the two is thought to arise from the difference in their non-stoichiometric characteristics [6] or it may be due to the contamination of free silicon or SiB_6 [7]. For this reason these compounds are termed "$SiB_{4\pm x}$" [8] in this paper.

SiB_6 was discovered in 1900 [1] when a mixture of silicon and boron was melted. The crystal structure of SiB_6 was initially reported to be cubic (CaB_6 type [9]), however, it was later confirmed to be orthorhombic Pnnm [10].

$SiB_{4\pm x}$ and SiB_6 are good candidate materials for a thermoelectric semiconductor [11], and have excellent potential as high-temperature materials [12, 13] because of their high oxidation and thermal shock resistances.

Some properties of $SiB_{4\pm x}$ and SiB_6 prepared by hot pressing have been reported in the past [11–13], but their intrinsic properties have been difficult to determine due to the existence of porosity, impurities and second phases.

Chemical vapour deposition (CVD) is a suitable method for preparing high-purity and high-density materials. Several reports on the CVD of the Si–B system have been published [14–19]. $SiB_{4\pm x}$ [14–17] and SiB_{14} [18, 19] in the shape of whiskers and thin films have been prepared; however, their properties have yet to be measured.

In the present work, by studying the effects of CVD conditions on morphology, structure and composition for the Si–B system, high-purity and high-density $SiB_{4\pm x}$ and SiB_6 plates about 1 mm thick were prepared.

2. Experimental procedure

A schematic diagram of the CVD apparatus is shown in Fig. 1. Silicon borides were prepared on the graphite substrates (40 mm × 12 mm × 2 mm) heated by an electric current using $SiCl_4$ vapour, B_2H_6 (5 vol %) + H_2 (95 vol %) mixture gas and H_2 gas. The deposition temperatures, T_{dep}, ranged from 1323–1773 K, the total gas pressures, P_{tot}, were varied from 4–40 kPa and the B/Si source gas ratio ($m_{B/Si} = 2B_2H_6/SiCl_4$) was controlled in the range 0.2–2.8. The deposition conditions are summarized in Table I.

The surface textures of the deposits were observed by SEM, and the crystal structures were examined by XRD (nickel-filtered, CuK_α). The compositions of the deposits were determined by chemical analysis and inductively coupled plasma analysis (ICP). The density was measured by the Archimedien method by immersion in toluene.

TABLE I Deposition conditions for the preparation of CVD $SiB_{4\pm x}$ and CVD SiB_6

Deposition temperature	1323–1773 K
Total gas pressure	4–40 kPa
Gas flow rate:	
$SiCl_4$	4.95×10^{-7}–16.8×10^{-7} $m^3 s^{-1}$
B_2H_6	1.67×10^{-7}–8.33×10^{-7} $m^3 s^{-1}$
H_2	2.0×10^{-5} $m^3 s^{-1}$
$2B_2H_6/SiCl_4$ ($m_{B/Si}$)	0.2–2.8
Deposition time	14.4 ks

0022–2461/92 $03.00 + .12 © *1992 Chapman & Hall*

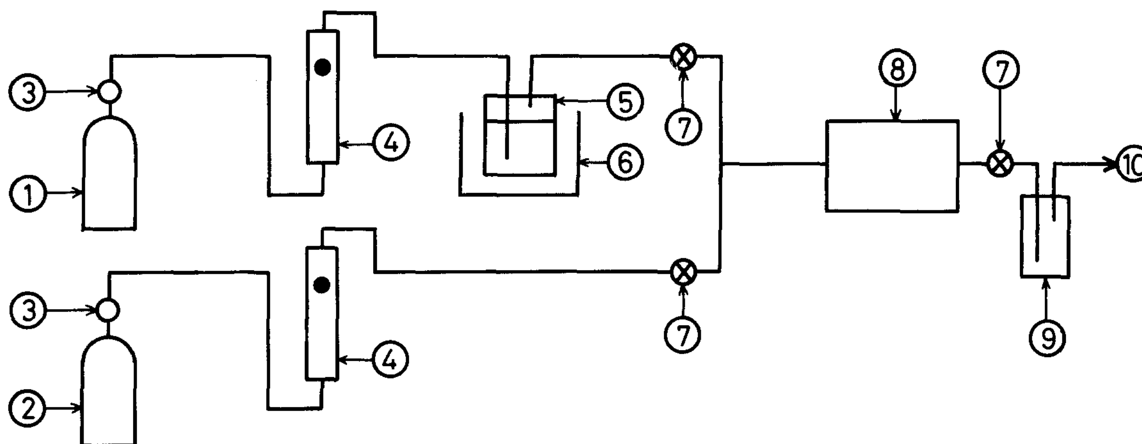

Figure 1 Schematic diagram of CVD apparatus for preparing $SiB_{4\pm x}$ and SiB_6 plates.
1, H_2 gas; 2, $B_2H_6 + H_2$ gas; 3, pressure regulator; 4, flow meter; 5, $SiCl_4$; 6, constant temperature bath; 7, valve; 8, reaction chamber; 9, cold trap; 10, rotary pump.

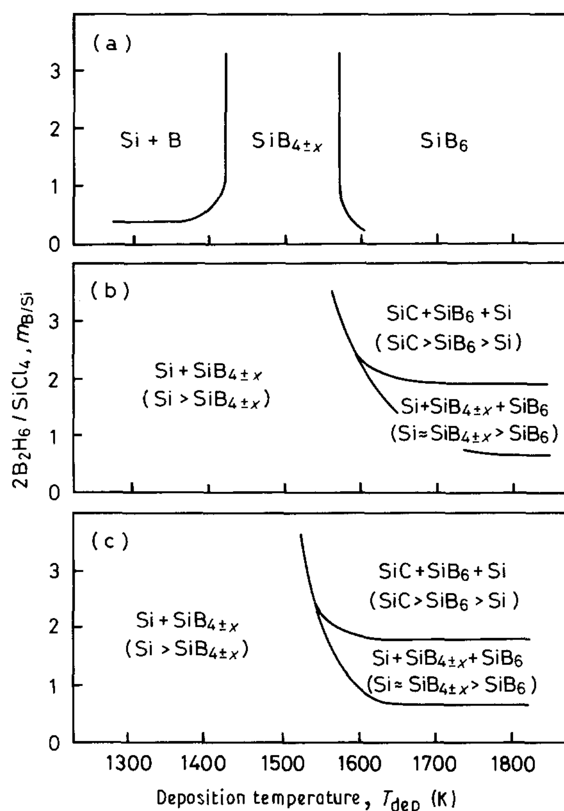

Figure 2 Effects of CVD conditions on the structures of deposits: (a) $P_{tot} = 4$ kPa; (b) $P_{tot} = 13$ kPa; (c) $P_{tot} = 40$ kPa.

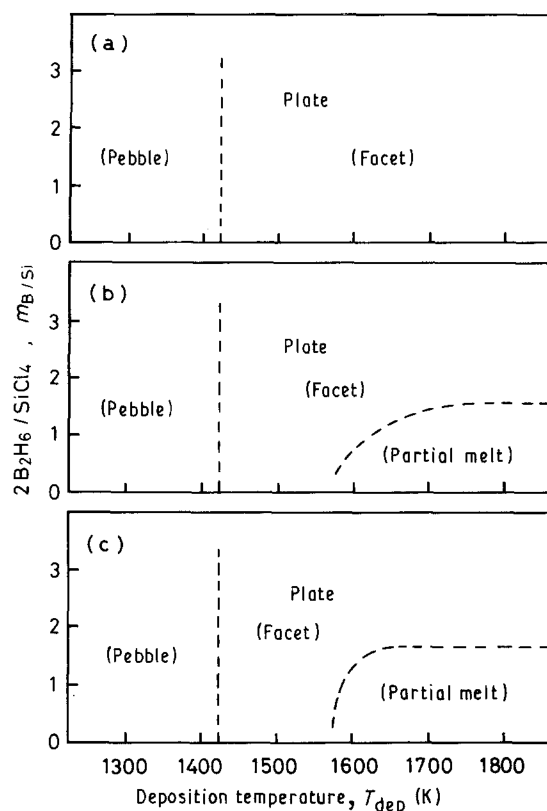

Figure 3 Effects of CVD conditions on the morphology of deposits: (a) $P_{tot} = 4$ kPa; (b) $P_{tot} = 13$ kPa, (c) $P_{tot} = 40$ kPa.

3. Results and discussion

Fig. 2 shows the effects of the CVD conditions on the structures of the deposits. The deposits prepared at $P_{tot} = 4$ kPa (Fig. 2a) were classified into three types: Si + B, $SiB_{4\pm x}$ and SiB_6. Both $SiB_{4\pm x}$ and SiB_6 were obtained in a single phase. The deposits prepared at both $P_{tot} = 13$ kPa (Fig. 2b) and 40 kPa (Fig. 2c) are classified into Si + $SiB_{4\pm x}$, Si + $SiB_{4\pm x}$ + SiB_6 and SiC + SiB_6 + Si. The X-ray diffraction analysis (XRD) showed that the contents of each phase prepared at $P_{tot} = 13$ and 40 kPa were Si > $SiB_{4\pm x}$ in the Si + $SiB_{4\pm x}$, Si = $SiB_{4\pm x}$ > SiB_6 in the Si + $SiB_{4\pm x}$ + SiB_6 and SiC > SiB_6 > Si in the SiC + SiB_6 + Si phases. The formation of SiC must be provoked by the reaction between the free silicon and graphite substrates. The free silicon was easily co-deposited when the total pressure exceeds 13 kPa, as shown in Fig. 2.

Fig. 3 shows the effects of CVD conditions on the morphology of the deposits. The morphology was classified into three groups; "pebble", "facet" and "partial melt". Fig. 4 shows typical surface textures observed by SEM for each group. It is well known that the morphology of CVD materials changes from "pebble" to "facet" with increasing T_{dep} [20]. The structure shown in Fig. 3 agrees with this well-known trend.

Fig. 5 shows an equilibrium phase diagram of the Si–B system [21, 22]. The diagram suggests the formation of a liquid phase when the deposition temperature exceeds 1658 K. Thus, the "partial melt" textures

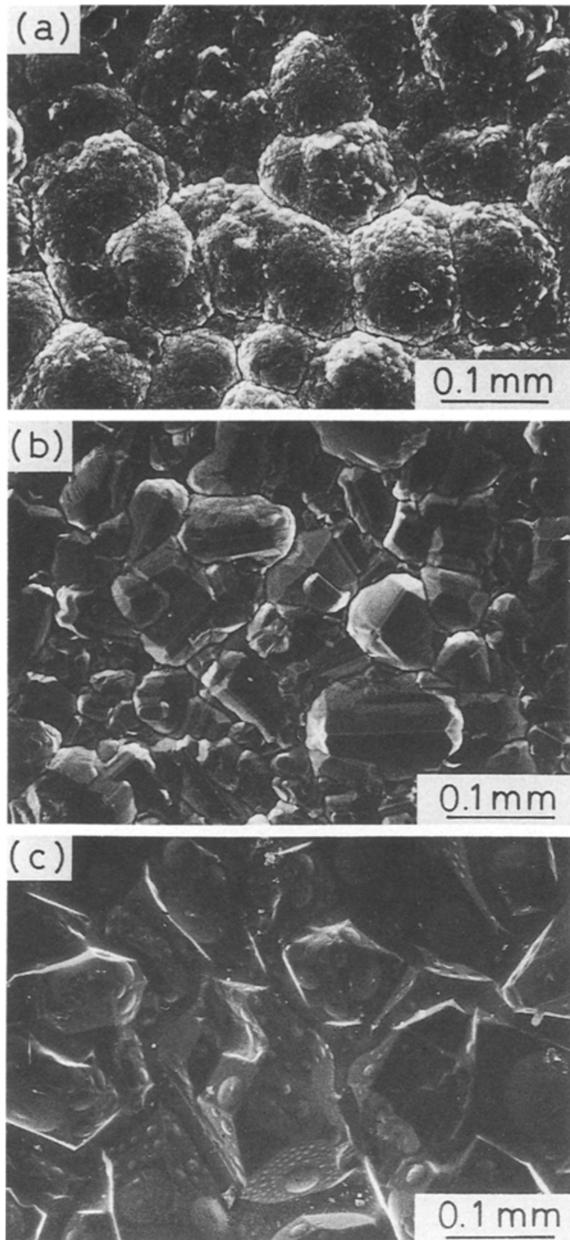

Figure 4 Typical surface textures of deposits: (a) pebble ($T_{dep} = 1373$ K, $P_{tot} = 4$ kPa, $m_{B/Si} = 0.2$); (b) facet ($T_{dep} = 1473$ K, $P_{tot} = 4$ kPa, $m_{B/Si} = 0.2$); (c) partial melt ($T_{dep} = 1573$ K, $P_{tot} = 13$ kPa, $m_{B/Si} = 0.2$).

shown in Figs 3 and 4 may be related to the characteristics of the equilibrium phase diagram. However, the equilibrium temperature for initiation of a liquid phase is about 100 K higher than the T_{dep} in the present work. This difference can be explained by two factors; first, the CVD may not be strictly in equilibrium, and second, the equilibrium phase diagram shown in Fig. 5 may not be a totally true phase diagram. The "partial melt" texture disappeared at higher $m_{B/Si}$, probably because almost all the liquid phase had reacted with graphite substrates to form SiC. According to the equilibrium phase diagram, $SiB_{4\pm x}$ becomes unstable at more than 1600 K and decomposes into SiB_6 and Si by the eutectic reaction

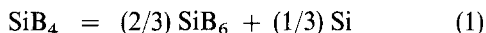

$$SiB_4 = (2/3)\,SiB_6 + (1/3)\,Si \qquad (1)$$

However, some papers [23, 24] reported that the eutectic temperature might be higher than 1643 K. These eutectic temperatures almost agree with the boundary of T_{dep} between the $SiB_{4\pm x}$ and SiB_6 regions shown in Fig. 2.

Figs 6 and 7 show the effect of $m_{B/Si}$ on the surface

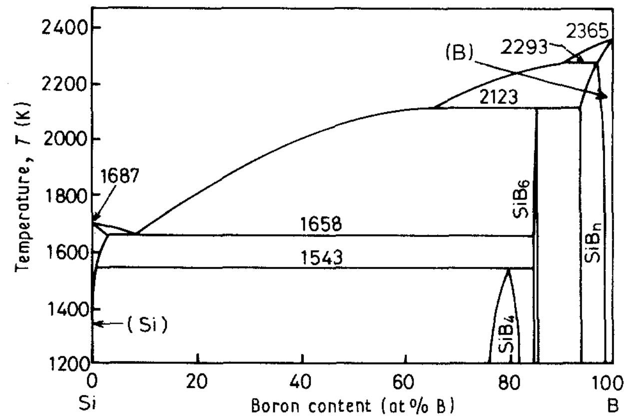

Figure 5 Equilibrium phase diagram of the Si–B system [20, 21].

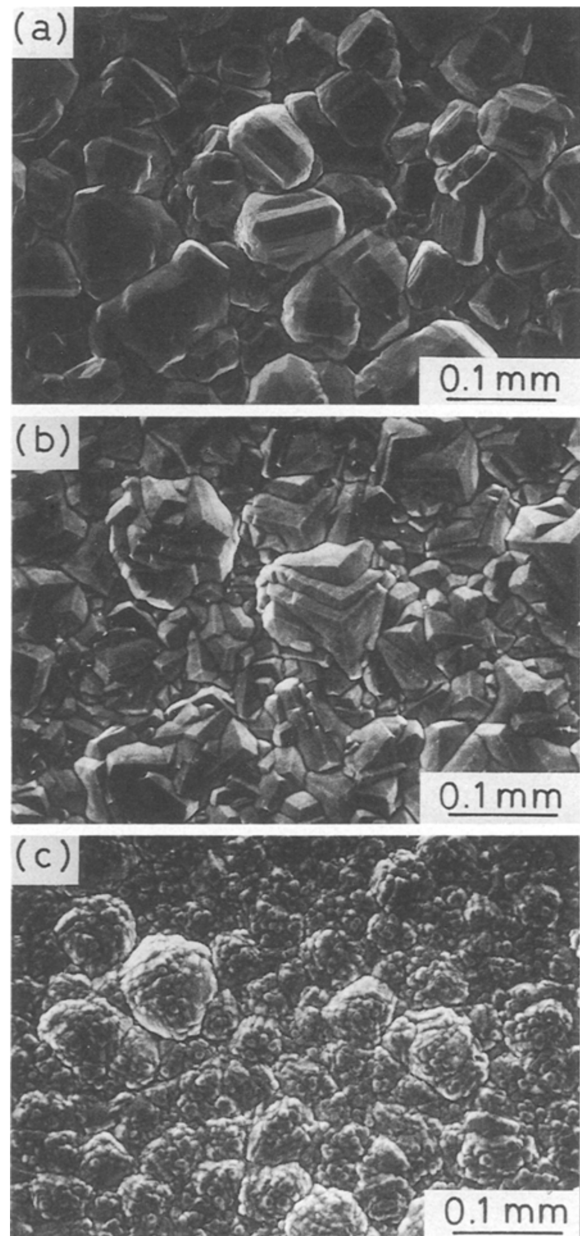

Figure 6 Effect of $m_{B/Si}$ on the surface textures of CVD $SiB_{4\pm x}$ plates prepared at $T_{dep} = 1473$ K, $P_{tot} = 4$ kPa: (a) $m_{B/Si} = 0.2$; (b) $m_{B/Si} = 0.8$; (c) $m_{B/Si} = 2.8$.

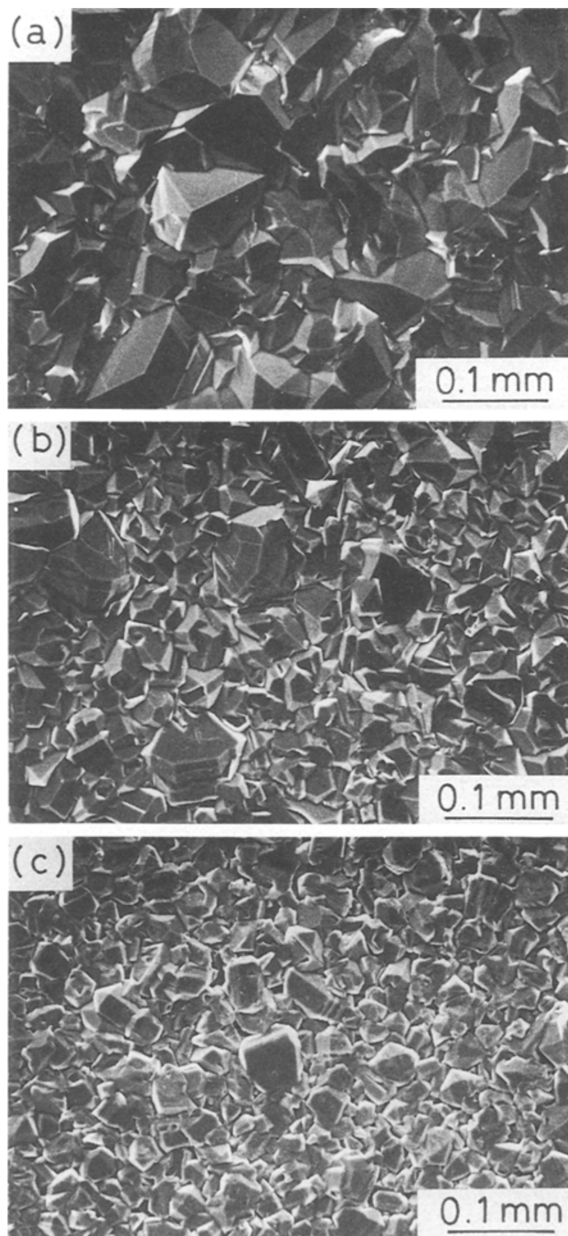

Figure 7 Effect of $m_{B/Si}$ on the surface textures of CVD SiB_6 plates prepared at $T_{dep} = 1473$ K, $P_{tot} = 4$ kPa: (a) $m_{B/Si} = 0.2$; (b) $m_{B/Si} = 0.8$; (c) $m_{B/Si} = 2.8$.

textures of CVD $SiB_{4\pm x}$ and CVD SiB_6 plates prepared at $P_{tot} = 4$ kPa, respectively. The grain size of both CVD $SiB_{4\pm x}$ and CVD SiB_6 plates decreased with increasing $m_{B/Si}$. It has been reported that the grain size of CVD TiB_2 [20] and CVD TiC [25] decreased with an increase of the boron and carbon source gas ratio. In general there is a common tendency of decreasing grain size with increasing source gas ratio of nonmetallic elements. When $m_{B/Si}$ becomes higher, a large amount of fine boron powder is formed in the gas phase, and these powders may become nucleation sites for crystal growth on the substrates. The smaller grain size observed at higher $m_{B/Si}$ can be explained in this manner.

Fig. 8a and b show the XRD patterns obtained from the powders of CVD $SiB_{4\pm x}$ and CVD SiB_6 plates, respectively. Free silicon and second phases were not detected, and they were both in a single phase.

Figs 9 and 10 show the effect of T_{dep} on lattice parameters of CVD $SiB_{4\pm x}$ and CVD SiB_6 plates, respectively. The CVD $SiB_{4\pm x}$ plates had a constant a value of 0.633 nm, while c values increased from 1.262–1.271 nm with increasing T_{dep}. The lattice parameters of CVD SiB_6 plates were all constant with $a = 1.444$ nm, $b = 1.828$ nm and $c = 0.9915$ nm, independent of CVD conditions.

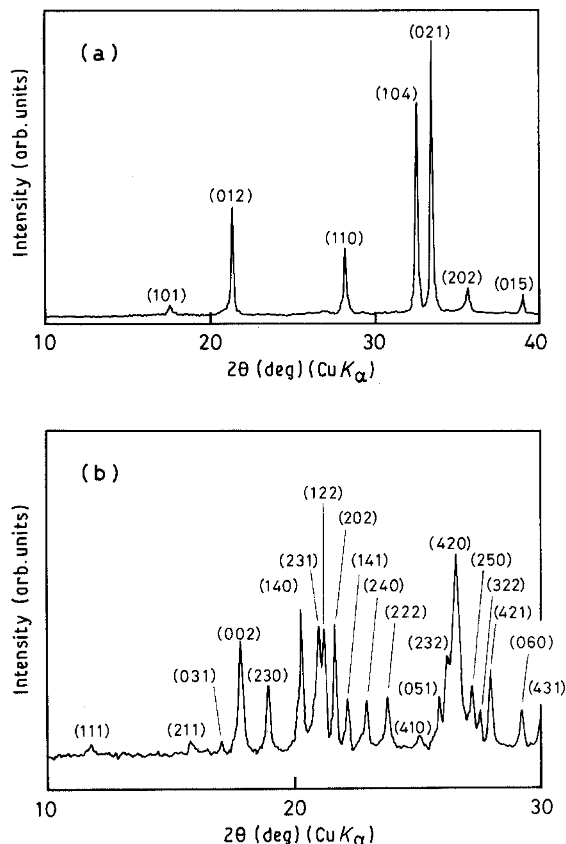

Figure 8 XRD powder patterns:
(a) CVD $SiB_{4\pm x}$ plate prepared at $T_{dep} = 1473$ K, $P_{tot} = 4$ kPa, $m_{B/Si} = 0.2$; (b) CVD SiB_6 plate prepared at $T_{dep} = 1673$ K, $P_{tot} = 4$ kPa, $m_{B/Si} = 0.8$.

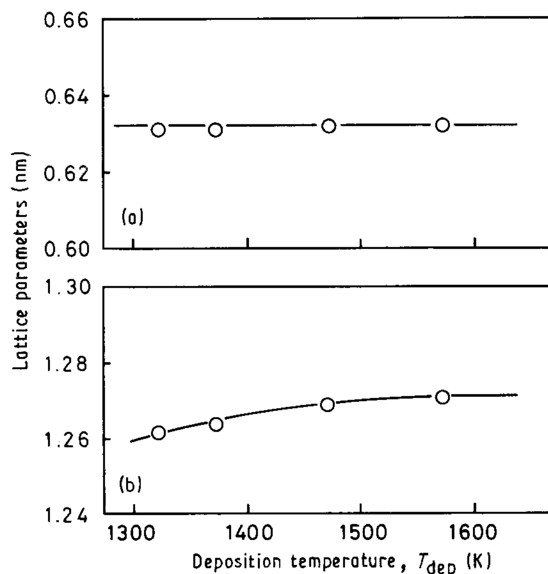

Figure 9 Effect of T_{dep} on the lattice parameters of CVD $SiB_{4\pm x}$ plates prepared at $P_{tot} = 4$ kPa, $m_{B/Si} = 0.2$. (a) a-axis, (b) c-axis.

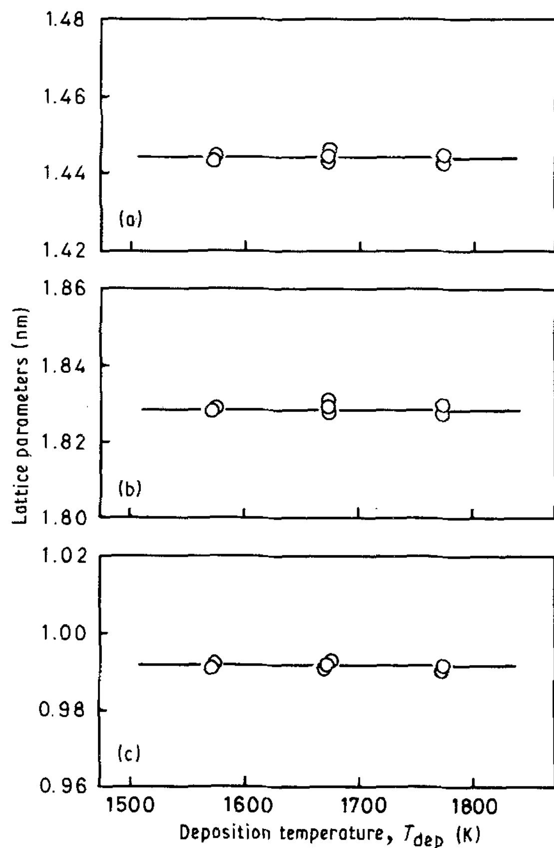

Figure 10 Effect of T_{dep} on the lattice parameters of CVD SiB_6 plates prepared at $P_{tot} = 4$ kPa, $m_{B/Si} = 0.8$. (a) *a*-axis, (b) *b*-axis, (c) *c*-axis.

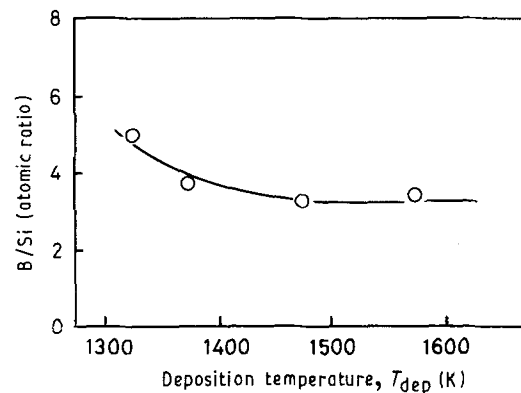

Figure 11 Effect of T_{dep} on the composition of CVD $SiB_{4\pm x}$ plates prepared at $P_{tot} = 4$ kPa, $m_{B/Si} = 0.2$.

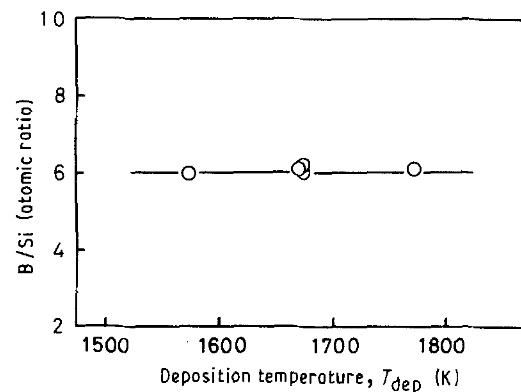

Figure 12 Effect of T_{dep} on the composition of CVD SiB_6 plates prepared at $P_{tot} = 4$ kPa, $m_{B/Si} = 0.8$.

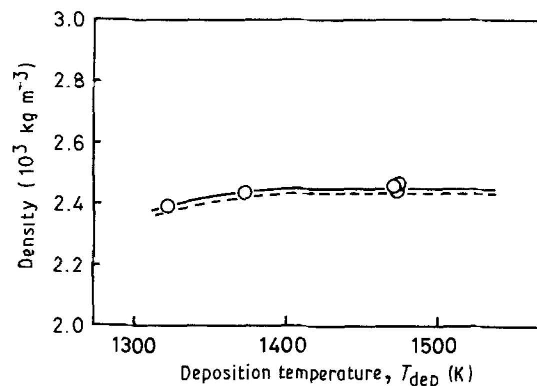

Figure 13 Effect of T_{dep} on the density of CVD $SiB_{4\pm x}$ plates prepared at $P_{tot} = 4$ kPa, $m_{B/Si} = 0.2$.

Figs 11 and 12 show the compositions of CVD $SiB_{4\pm x}$ and CVD SiB_6 plates, respectively. The B/Si atomic ratio of CVD $SiB_{4\pm x}$ plates decreased from 5.0 to 3.1 with increasing T_{dep}, while that of CVD SiB_6 plates had the constant value of 6.0.

The crystal structure of $SiB_{4\pm x}$ has been explained as being similar to that of B_4C, consisting of the space group of D^5_{3d}-R3m [6, 26]. B_4C is known to have a wide non-stoichiometric range between B/C = 3.6 and 10.8 [27, 28]. With the non-stoichiometric composition of B_4C when B_4C exists with excess boron, the three inter-icosahedron carbon sites are partially substituted by boron atoms, while for excess carbon in B_4C, the 20 intra-icosahedron boron sites are partially substituted by carbon atoms [28–31]. The same reasoning can be applied to illustrate the non-stoichiometry of $SiB_{4\pm x}$ [6, 26]. Thus, the difference in non-stoichiometry characteristics must be contributing to the observed variations of lattice parameters and compositions of CVD $SiB_{4\pm x}$ plates with T_{dep}, as shown in Figs 9 and 11.

It is known that SiB_6 has the structure of orthorhombic P n n m [10] and may have a non-stoichiometric composition range of between B/Si = 5.7 and 6.1 [10]. However, many past reports [32, 33], as well as the present work, have shown that SiB_6 may be a stoichiometric compound.

Fig. 13 shows the effect of T_{dep} on the density of CVD $SiB_{4\pm x}$ plates. The density increased from 2.39×10^3 to 2.45×10^3 kg m^{-3} with increasing T_{dep}. The broken line in Fig. 13 shows calculated values based on the following assumptions: when the B/Si atomic ratio is more than 4, the three inter-icosahedron silicon sites are partially substituted by boron atoms, and when the B/Si atomic ratio is less than 4, the 20 intra-icosahedron boron sites are partially substituted by silicon atoms as mentioned earlier. The calculated results are in good agreement with the experimental data.

Fig. 14 shows the effect of T_{dep} on the density of CVD SiB_6 plates. The density of CVD SiB_6 plates remained constant (2.42×10^3 kg m^{-3}), and agreed with the theoretical value (2.418×10^3 kg m^{-3}).

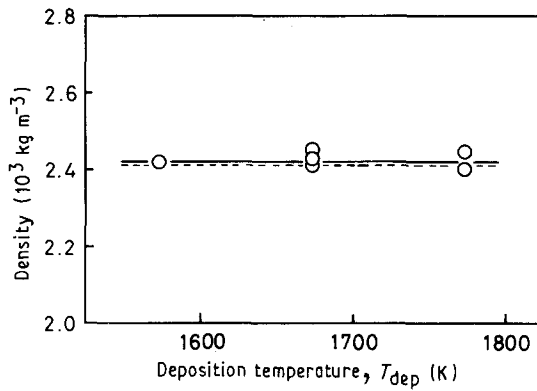

Figure 14 Effect of T_{dep} on the density of CVD SiB_6 plates prepared at P_{tot} = 4 kPa, $m_{B/Si}$ = 0.8.

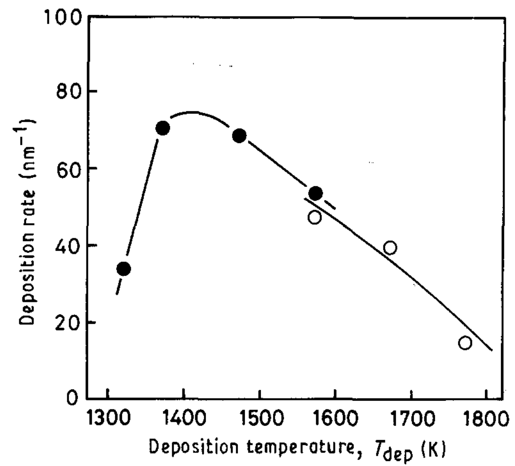

Figure 15 Effect of T_{dep} on the deposition rates of (●) CVD $SiB_{4\pm x}$ plates ($m_{B/Si}$ = 0.2) and (○) CVD SiB_6 plates ($m_{B/Si}$ = 0.8) prepared at P_{tot} = 4 kPa.

Tables II and III summarize the lattice parameters, composition and density of $SiB_{4\pm x}$ (Table II) and SiB_6 (Table III) prepared by various techniques.

Fig. 15 shows the effect of T_{dep} on the deposition rates of CVD $SiB_{4\pm x}$ and CVD SiB_6 plates. The deposition rate of CVD $SiB_{4\pm x}$ plates had a maximum value of 71 nm s^{-1} (256 μm h^{-1}) at T_{dep} = 1373 K, P_{tot} = 4 kPa and $m_{B/Si}$ = 0.2. The deposition rate of CVD SiB_6 plates continuously decreased with increasing T_{dep}. The largest value was 47 nm s^{-1} (170 μm h^{-1}) at T_{dep} = 1573 K, P_{tot} = 4 kPa and $m_{B/Si}$ = 0.8. The reason for this decrease in deposition rate with increasing T_{dep} may be due to the powder formation by homogeneous reactions in the gas phase, as mentioned earlier.

Table IV summarizes the properties of silicon borides prepared by CVD in the previous [14, 15, 17–19] and present work. There are no known reports on the

TABLE II Lattice parameter, density and composition of CVD $SiB_{4\pm x}$

Method	Lattice parameter (nm)	Density (10^3 kg m^{-3})	Composition (B/Si)	Reference
Sintering	a = 0.5319 c = 1.2713	2.44	2.89	[6]
	a = 0.632 c = 1.275	2.46	2.96	[26]
	a = 0.6330 c = 1.2736	2.47	4.27	[7]
CVD	a = 0.628 c = 1.272			[15]
	a = 0.633 c = 1.262–1.271	2.39–2.45	3.1–5.0	Present work

TABLE III Lattice parameters, density and composition of CVD SiB_6

Method	Lattice parameter (nm)	Density (10^3 kg m^{-3})	Composition (B/Si)	Reference
Fusion	a = 1.460 b = 1.840 c = 1.002	2.45	5.9	[3]
	a = 1.4392 b = 1.8267 c = 0.9885	2.43	6.1	[32]
	a = 1.439 b = 1.827 c = 0.988	2.43	6.0	[33]
	a = 1.4397 b = 1.8318 c = 0.9923	2.42		[10]
CVD	a = 1.444 b = 1.828 c = 0.992	2.42	6.0	Present work

TABLE IV Deposition conditions and some properties of silicon borides prepared by CVD

Reactants	Deposition conditions			B/Si	Morphology	Thickness (mm)	Reference
	T_{dep} (K)	P_{tot} (kPa)	$m_{B/Si}$				
$SiCl_4 + BBr_3$	1423		0.33	3	Wire coating	–	[15]
$SiCl_4 + BCl_3$	1223–1473		0.5–2	4	Whisker	–	[14]
$SiH_4 + BCl_3$	1073–1673	6.7–8.0	2–5	4	Film	0.005 ~ 0.3	[17]
$SiBr_4 + BBr_3$	1200–1800	6.7×10^{-3}	1–14	14	Film	0.2 ~ 0.3	[18]
$SiBr_4 + BBr_3$	1200–1600	6.7×10^{-3}	12–20	14	Film	0.05	[19]
$SiCl_4 + B_2H_6$	1323–1573	4	0.2–2.8	$4 \pm x$	Plate	1.0	Present work
$SiCl_4 + B_2H_6$	1573–1773	4	0.2–2.8	6	Plate	0.7	Present work

preparation of SiB_6 by CVD except for the present work. The thickness of CVD $SiB_{4\pm x}$ plates obtained in the present work was about 1 mm at most. This value is about 3–200 times larger than those previously reported. Up to now only one known report on the deposition rate of silicon borides (SiB_{14}) was available [18]. According to this report the deposition rate of CVD SiB_{14} was $30\ \mu m\ h^{-1}$ at $T_{dep} = 1520$ K [18].

In the present work, the cold-wall-type CVD furnace was used and fresh source gases were transported to the heated substrates with minimum premature reactions. These factors may have contributed to the deposition of very thick CVD $SiB_{4\pm x}$ and CVD SiB_6 plates at higher deposition rates.

4. Conclusions

$SiB_{4\pm x}$ and SiB_6 plates were prepared by CVD using $SiCl_4$, B_2H_6 and H_2 gases under the conditions of $T_{dep} = 1323$–1773 K, $P_{tot} = 4$–40 kPa and $m_{B/Si} = 0.2$–2.8. The following results were obtained.

1. When $P_{tot} = 4$ kPa and $T_{dep} < 1573$ K, $SiB_{4\pm x}$ plates were obtained. When $P_{tot} = 4$ kPa and $T_{dep} > 1573$ K, SiB_6 plates were obtained. Both plates were in a single phase. When $P_{tot} > 13$ kPa, free silicon was co-deposited in both CVD $SiB_{4\pm x}$ and CVD SiB_6 plates independent of T_{dep} and $m_{B/Si}$.

2. The grain size of CVD $SiB_{4\pm x}$ and CVD SiB_6 plates decreased with increasing $m_{B/Si}$. The formation of fine boron powder in the gas phase becomes more noticeable with higher $m_{B/Si}$. This boron powder may become nucleation sites on the substrate surface.

3. The CVD $SiB_{4\pm x}$ plates had a non-stoichiometric composition range between B/Si = 3.1 and 5.0. The lattice parameter and density varied depending on the non-stoichiometry. The lattice parameter, a, was constant at 0.6325 nm, but c ranged from 1.262–1.271 nm. The density changed from 2.39–$2.45 \times 10^3\ kg\ m^{-3}$.

4. The CVD SiB_6 plates had constant values of lattice parameter ($a = 1.444$ nm, $b = 1.828$ nm and $c = 0.9915$ nm), composition (B/Si = 6) and density ($2.42 \times 10^3\ kg\ m^{-3}$), independent of CVD conditions.

5. The maximum deposition rate of CVD $SiB_{4\pm x}$ and CVD SiB_6 plates was $71\ nm\ s^{-1}$ (at $T_{dep} = 1373$ K, $P_{tot} = 4$ kPa and $m_{B/Si} = 0.2$), while for CVD SiB_6 plates it was $47\ nm\ s^{-1}$ (at $T_{dep} = 1573$ K, $P_{tot} = 4$ kPa and $m_{B/Si} = 0.8$). The maximum thickness of any plates was about 1 mm.

Acknowledgements

The authors thank Mr Narushima, Faculty of Engineering, Tohoku University, for the ICP analysis. This research was supported in part by the Grant-in-Aid for Scientific Research under Contract no. 01 550 543 from the Ministry of Education, Science and Culture.

References

1. H. MOISSAN and A. STOCK, *Compt. Rend.* **131** (1900) 139.
2. E. COLTON, *J. Amer. Chem. Soc.* **82** (1960) 1002.
3. C. F. CLINE, *Nature* **15** (1958) 476.
4. R. F. GIESE Jr, J. ECONOMY and V. I. MATKOVICH, *Z. Kristallogr.* **122** (1965) 144.
5. C. F. CLINE and D. E. SANDS, *Nature* **185** (1960) 456.
6. B. MAGNUSSON and C. BROSSET, *Acta Chem. Scand.* **16** (1960) 449.
7. V. I. MATKOVICH, *Acta Crystallogr.* **13** (1960) 679.
8. T. GOTO, M. MUKAIDA and T. HIRAI, in Symposium Proceedings, "Chemical Vapor Deposition", Boston, November 1989, edited by T. M. Besmann and B. Gallois (Materials Research Society, Pittsburgh, PA, 1990) in press.
9. N. N. ZHURAVLEV, *Kristallogr.* **1** (1956) 666.
10. M. VLASSE, G. A. SLACK, M. GARBAUSKAS, J. S. KASPER and J. C. VIALA, *J. Solid State Chem.* **63** (1986) 31.
11. C. WOOD, D. EMIN, R. S. FEIGELSON and I. D. R. MACKINON, in Symposium Proceedings, Vol. 97, "Novel Refractory Semiconductors", California, April 1987, edited by D. Emin, T. L. Aselage and C. Wood (Materials Research Society, Pittsburgh, PA, 1987) p. 33.
12. H. F. RIZZO, B. C. WEBER and M. A. SCHWARTZ, *J. Amer. Ceram. Soc.* **43** (1960) 497.
13. R. S. FEIGELSON and W. D. KINGERY, *Amer. Ceram. Soc. Bull.* **42** (1963) 688.
14. S. MOTOJIMA, K. SUGIYAMA and Y. TAKAHASHI, *Bull. Chem. Soc. Jpn* **48** (1975) 1463.
15. I. V. PETRUSHERICH, L. A. NISEL'SON, A. I. BELYAEV and M. A. GUREVICH, *Izv. Akad. Nauk SSR. Neorg. Mater.* **3** (1967) 1389.
16. C. POWELL and I. CAMPBELL, *Monatsh. Chem.* **88** (1957) 180.
17. R. R. DIRKX and K. E. SPEAR, "Emergent Process Methods for High-Technology Ceramics", Materials Science Research, Vol. 17, edited by R. F. Davis, H. Palmour III and R. L. Porter (Plenum, New York, 1982) p. 359.
18. B. ARMAS, C. COMBESCURE, J. M. DUSSEAU, T. P. LEPETRE, J. L. ROBERT and B. PISTOULET, *J. Less-Common Metals* **47** (1976) 135.
19. B. ARMAS and C. COMBESCURE, in "Proceedings of the 6th International Conference on Chemical Vapor Deposition", Atlanta, October 1977, edited by L. F. Donaghey, P. Rai-Choudhury and R. N. Tauber (Electrochemical Society, Princeton, NJ, 1977) p. 181.
20. M. MUKAIDA, T. GOTO and T. HIRAI, *J. Mater. Sci.* **25** (1990) 1069.
21. R. W. OLESINSKI and G. J. ABBASHIAN, *Bull. Alloy Phase Diagram* **5** (1984) 478.

22. B. ARMAS, G. MALE, D. SALANOUBAT, C. CHATILLON and M. ALLIBERT, *J. Less-Common Metals* **82** (1981) 245.
23. E. COLTON, *J. Inorg. Nucl. Chem.* **17** (1961) 108.
24. L. KAUFMANN, B. UHRENIUS, D. BIRNIE and K. TAYLOR, *Calphad* **8** (1984) 25.
25. C. JIANG, T. GOTO and T. HIRAI, *J. Mater. Sci.* **25** (1990) 1086.
26. H. F. RIZZO and L. R. BIDWELL, *J. Amer. Ceram. Soc.* **43** (1960) 550.
27. M. BEAUVY, *J. Less-Common Metals* **90** (1983) 169.
28. I. A. HOWARD, C. L. BECKEL and D. EMIN, in Symposium Proceedings, Vol. 97, "Novel Refractory Semiconductors", California, April 1987, edited by D. Emin, T. L. Aselage and C. Wood (Materials Research Society, Pittsburgh, PA, 1987) p. 39.
29. C. WOOD and D. EMIN, *Phys. Rev.* **B29** (1984) 4582.
30. M. V. VLASOVA, N. G. KAKAZEY, T. Y. KOSOLAPOVA, G. N. MAKARENKO, E. V. MAREK, D. USKOKOVIC and M. M. RISTIC, *J. Mater. Sci.* **15** (1980) 1041.
31. F. W. GLASER, D. MOSKOWITZ and B. POST, *J. Appl. Phys.* **24** (1953) 731.
32. R. F. ADAMSKY, *Acta Crystallogr.* **11** (1958) 744.
33. C. F. CLINE, *J. Electrochem. Soc.* **106** (1959) 322.

Received 3 September 1990
and accepted 28 February 1991